Comparison of Coupling Coefficient and Magnetic Field Distribution of Contactless Transformer

Abdul Jabbar F. Ali / Wasit University / College of Engineering

Abstract

The direct – switched apparatus in use nowadays are connected to the mains through plugs and sockets. These are generally agreed in natural environment, but can be prohibited or have limited life in the presence of moisture, in explosive atmospheres and inside sea applications. So contactless power transmission through a large air-gap is becoming more suitable for the above applications. This paper discusses the effects of geometrical arrangements of contactless transformer for two core types, U-U type and E-E type by means of flux simulation based on finite element method with ANSYS program v 5.4 . It is found that the U-U type core can give higher coupling coefficient within the same core geometry and lower leakages. It could be concluded that the dimensions of the core and the air-gap length determine the transmission behavior.

1. Introduction

Isolation and load supply voltage are the main applications of a magnetic transformer. If the primary and secondary winding of the transformer are wound on separate magnetic core, then energy coupling possible without physical connection between the source and load units. Some applications are robots, machine tools, linear rotatable system and non-contact battery charger for electric vehicles [1, 2, 3]. Contactless transmission technology for trailing cables can be replaced and therefore cable breaks can be avoided. Other advantages are: no deterioration on the electrical contacts, no contact resistance, no sparking (can be applied in explosion-environment) and no non-protected voltage – carrying contacts [4, 5]. The transformer core design for the maximum coupling coefficient with the size constraint on the secondary side is presented. Two types of cores geometries are discussed. An equivalent magnetic model is applied to derive qualitatively the coupling coefficient K as a function of core geometry and air-gap length.

2. Modeling And Analysis of Contactless Transformer

The schematic diagram of the contactless transformer is shown in Fig.1. Two types of core shape are used. One type has a center pole, such as E-E type pot core, and the other has no center pole such as U-U type. The two core types are shown in Fig.2. The relative permeability of the ferrite core is much larger than that of the air.
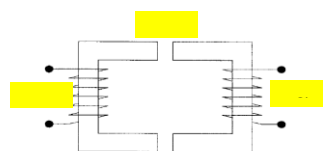

Fig.1 The contactless transformer with separated Core structure.

Therefore, the reluctance of the ferrite core can be ignored. The leakage flux is mainly due to the RU_2, RU_3 in the U-U type and RE_2 in the E-E type as shown in Fig.3. RU_1 and RE_3 represent the reluctance of the air-gap.

In order to obtain the coupling coefficient K, the equivalent magnetic circuits are used. The coupling coefficient of the U-U type is derived from the fundamental definitions .
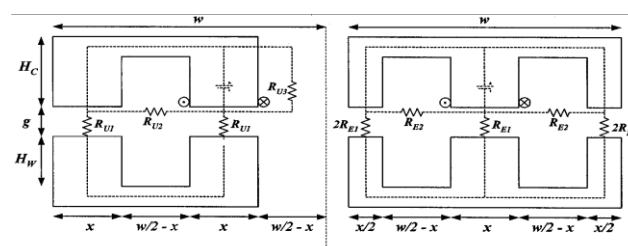

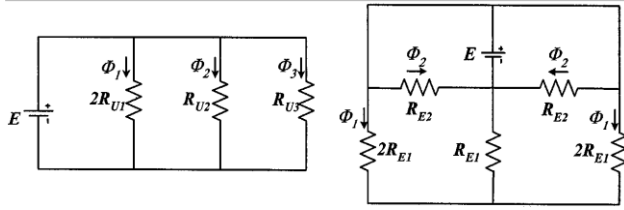Fig.2: Core shape and the reluctances of the U-U type and E-E type

Fig.3: Equivalent magnetic circuit of (a) U-U type (b) E-E type

$$K = \frac{\Phi_1}{\Phi_1 + \Phi_2 + \Phi_3} \qquad \text{------------ (1)}$$

Equation (1) can be replaced with the reluctances.

Then,

$$K = \frac{\dfrac{E}{2RU_1}}{\dfrac{E}{2RU_1} + \dfrac{E}{RU_2} + \dfrac{E}{RU_3}} \qquad \text{-------------- (2)}$$

In the same manner, the coupling coefficient of the E-E type can be obtained:

$$K = \frac{\Phi_1}{\Phi_1 + \Phi_2} \qquad \text{--------------- - (3)}$$

$$K = \frac{\dfrac{E}{4RE_1}}{\dfrac{E}{4RE_1} + \dfrac{E}{RE_2}} \qquad \text{---------------- - (4)}$$

RU_2 , RU_3 and RE_2 are drawn in Fig. 4 as against pole width x. The total width w of the U-U type is maintained as same as that of E-E type. From Fig.3 RU_3 remains almost constant for the varying pole width x, but RU_2 and RE_2 decrease rapidly for (x>11 mm). That is because of the distance between the poles becomes smaller as x becomes larger.

For comparing the two types, the coupling coefficients K are drawn as a function of the core weight. In Fig.5. The coupling coefficients of the two types are similar for the same pole width x when (x<11 mm) and the coupling coefficient of the U-U type becomes higher when (x>11 mm). Also the core geometry of the U-U type is smaller than that of the E-E type at the same pole width x, therefore the U-U type can give higher coupling coefficient within the same core weight as shown in Fig.5. Fig.6 shows the coupling coefficient as a function of the

ratio of the total width w to the gap length g in order to obtain information for the total width. The two types have similar coupling coefficient and the slope of K becomes lower when the ratio (w/g) exceeds approximately by 10 [6, 7].

3. Magnetic Vector Potential formulation:

The Maxwell's equations are applied and solved with the help of the program. The results include magnetic field intensity, magnetic flux density, magnetic forces and current densities. The magnetic vector potential methods is applied for such evaluation. The magnetic flux density is the first derived result it is defined as the curl of the magnetic vector potential. This evaluation is performed at the integration points using the element shape function given in [8 , 9]:

$$\{B\} = \nabla X \, [N_A]^T \{A_e\} \qquad \text{-------------- (5)}$$

Where: {B} = Magnetic flux density

$\qquad \nabla X$ = Curl operator

$\qquad [N_A]$ = Shape functions

$\qquad \{A_e\}$ = Nodal magnetic vector potential

Then the magnetic field intensity is coupled from the flux density:

$$\{H\} = [V] \, \{B\} \qquad \text{--------------- (6)}$$

Where: {H} = Magnetic field intensity

$\qquad$ [V] = Reluctivity matrix

Nodal values of field intensity and flux density are computed from the integration point value.

4. Maxwell Forces:

It is well known that parallel conductors will repel or attract each other according whether the currents they carry are in the opposite or on the same direction. Forces exist in ordinary transformers, the cause being the interaction of currents in the winding with the leakage

field surrounding them and along the surface of the transformer. The magnitude of the force on a conductor of the transformer is proportional to the product of the current in it and the intensity of the magnetic field due to neighboring currents , and since the latter itself proportional to the current , the forces per unit length of the magnetic circuit is proportional to the square of the current. The Maxwell stress tensor is used to determine forces on ferromagnetic regions. For the 2-D application, this methods used extrapolated field values and results in the following numerically integrated surface integral [10]:

$$\{F^{mx}\} = \frac{1}{\mu_0} \int_s \begin{bmatrix} T_{11} & T_{12} \\ T21 & T_{22} \end{bmatrix} \begin{Bmatrix} n_1 \\ n_2 \end{Bmatrix} ds \quad \text{------- (7)}$$

Where : μ_0 = Permeability of free space

$$T_{11} = B_x^2 - \frac{1}{2}|B|^2$$

¶ $$T_{21} = T12 = B_x B_y$$

$$T_{22} = B_y^2 - \frac{1}{2}|B|^2$$

n_1, n_2 are unit normal , n =

The electromagnetic field evaluation results are discussed in the following section:

5. Simulation Results And Discussion :

The magnetic flux production is   assumed to be so small that no saturation of the core occurs. The air-gap is modeled so that a quadrilateral mesh is possible. A quadrilateral mesh for uniform thickness of the air elements adjacent to the coil where the virtual work force calculation is performed. This is desirable for an accurate force calculation. The software used was the finite – element method of ANSYS V. 5.4. The program requires that the current to be input in the form of current density (current over the area of the coil). As a result of simulation Fig.7 and Fig.8 show simulated distribution of the magnetic flux lines in the air-gap and the core, where certain amount of flux leakage occurs out of the core for

both the U-U type and E-E type respectively. While Fig.9 and Fig.10 show the distribution of the flux density B as vectors distributed throughout the entire core. Fig.11 and Fig.12 show the magnitude of the magnetic field intensity without averaging the results across material discontinuities. Up to this point, the analysis and all associated plots have used 2-D plane model, with the axis of symmetry aligned with the left vertical portion of the device. The field simulation considers both the skin and the proximity effects. Because of the skin effect, the current concentrates in a layer near the surface of the conductor. The second effect within this case is the proximity effect which results in an inhomogeneous current distribution over the wire perimeter. The summary of forces by Maxwell stress tensor are as follows:

Units of force: N/m

Component: Force – X   Force--Y

Secondary: -0.36054 E-04   -0.9476E-02

Note: Maxwell forces are in the global Cartesian coordinate system. The forces correspond to a full 360 degree revolution of the cross – section (of planner model).

6. Conclusions :

The two types of contactless transformer has been modeled and presented. The analysis of the U-U type and the E-E type were performed and analyzed in order to get a better coupling coefficient K under the size and gap variation. The U-U type offer a higher coupling coefficient than the E-E type arrangement at the same core weight. The simulated results of the main inductances and leakage inductances of contactless transformers mainly depend on the dimensions of the primary and secondary windings, the existence of ferrite cores on the primary or secondary side and the air-gap length. The analysis of the contactless transformer and all associated plots have used the 2-D plane model, with the axis of symmetry aligned with the left vertical portion of the device. The field simulation calculations consider both the skin and the proximity effects on the conducting parts.

References

1- K. Lashkari, S.E. shladover, "Inductive power transfer to an electric vehicle" , in proc. 8th Int. Electric Vehicle symp. 1986. pp. 258-267.

2- F. Sato, J. Murakami, "Contactless energy transmission to mobile loads by CLPS-Test driving an electic vehicle with starter batteries, "IEEE Trans. Magn, Vol. 33, pt. 2 , pp. 4203 – 4205, 2001.

3- B.J Heeres, D.W. Novotny, "Contactless underwater power delivery". In proc. IEEE Pesc 94, 2002 Vol. 1 , pp. 418-423.

4- D.A.G. Pedder, A.D. Brown, "A contactless electrical energy transmission system" . IEEE Trans. Ind Electron, Vol. 46, pp. 23-30 Feb. 1999.

5- A. Esser and H. Skudelny, "A new approach to power supplies for robots, "IEEE Trans. Ind Applicate, Vol 27 , pp. 872-875, Sept/oct. 1999.

6- K.W. lontz, D.M. Divan, "Contactless power delivery system for mining applications". IEEE Trans. Ind application, Vol. 31, pp. 27-35. Jan/Feb 1995.

7- Wu Ying, Yan Luguan and Xu Shangan, " New Contactless Power Transmission System " , Bianygi , Vol. 40 , No. 6 , June 2014 , pp. 1-6.

8- Myunghyo Ryu , Honn Yong Cha. , Yonghwan Park , " Analysis of the Contactless Power Transfer System Using Modeling and Analysis of the Contactless Transformer " IEEE Trans. On Power Electronics, 2012 ,pp. 1036 – 1042 .

9- Hui S.Y.R and Ho, C.W.W. " A New Generation of Universal Contactless Battery Charging Platform For Portable Consumer Electronic Equipment", IEEE Trrans. On Power Electron, Vol. 20 ,No. 3 , May 2013.

10- Jang Y, and Jovanovic M. M., " A Contactless Energy Transmission
 System For Portable - Telephone Battery Charger " IEEE Trans.
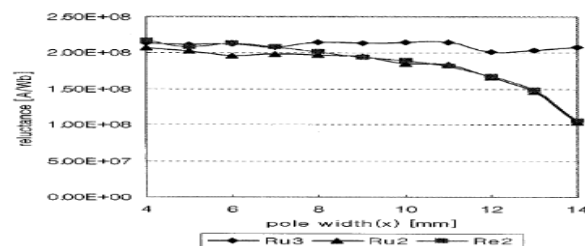   Ind . Electron. Vol. 50, No.3, Jun 2011,pp. 520-527.
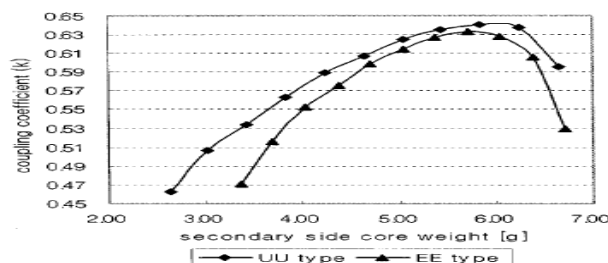
Fig.4 Reluctances of the magnetic circuit (RU2,RU3,RE2).

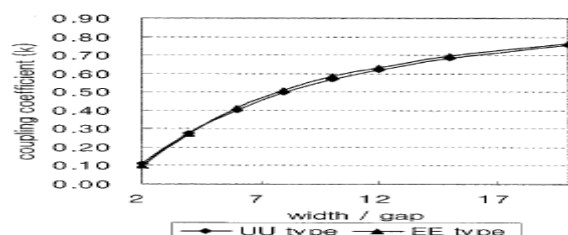**Fig.5 Coupling coefficient K as a function of core weight**

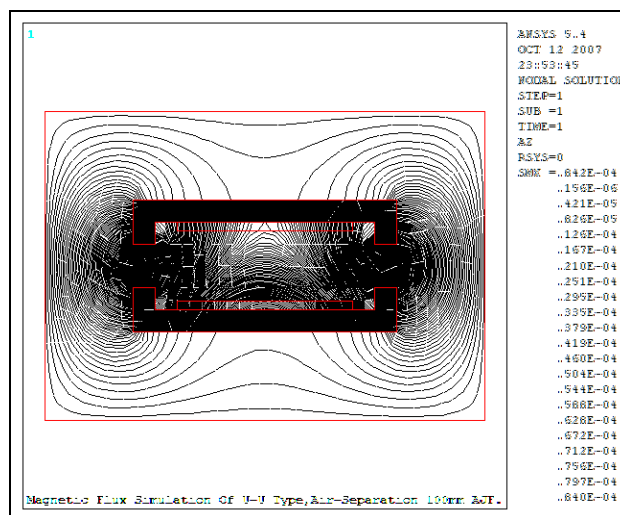**Fig.6 Coupling coefficient K as a function of the ratio (w/g) of the width (w) and the gap length (g).**

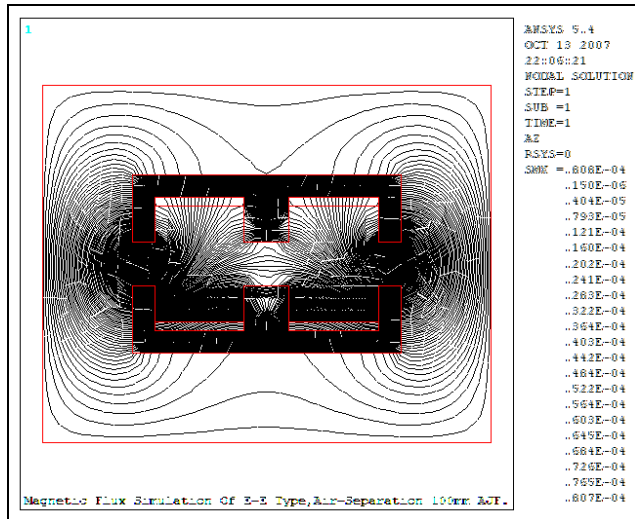**Fig. 7 : Simulated distribution of magnetic flux lines of U-U type core.**

Fig. 8 : Simulated distribution of magnetic flux lines of E-E type core.
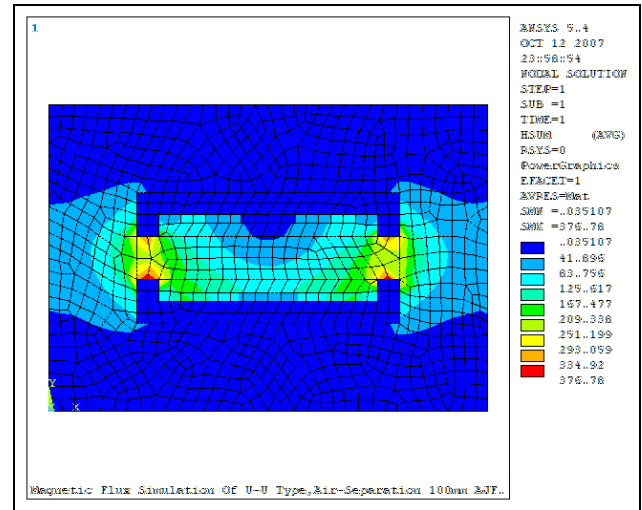

Fig. 11 : Simulated distribution of contours plot of magnetic field intensity Hsum of U-U type core.
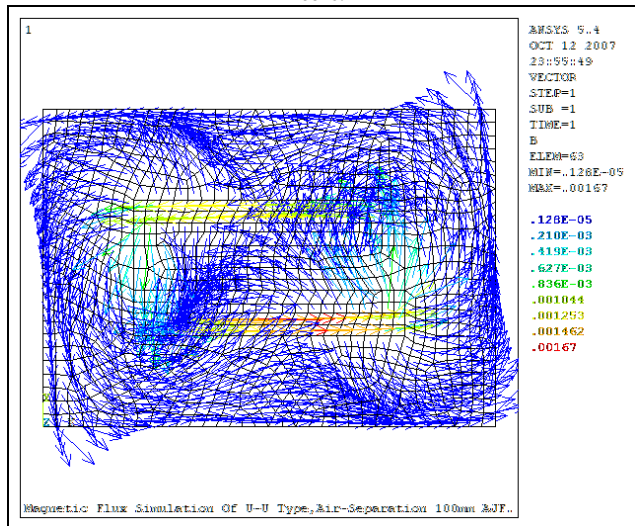

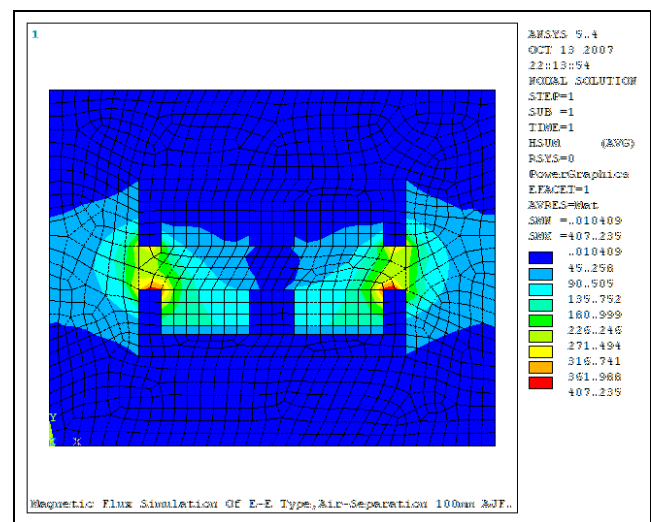**Fig. 9 : Simulated distribution of vector plots of magnetic flux density B of U-U type core.**

Fig. 12 : Simulated distribution of contours plot of magnetic field intensity H.sum of E-E type core.
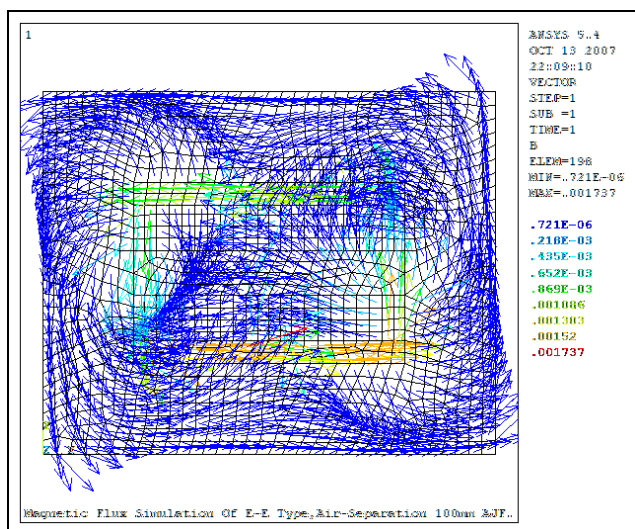

Fig. 10 : Simulated distribution of vector plots of magnetic flux density B of U-U type core.